How to cite: *Angew. Chem. Int. Ed.* **2023**, *62*, e202307352
doi.org/10.1002/anie.202307352

C-C Bond Formation | Hot Paper

Evidence for Carbene Intermediates in Isocyanide Homologation by Aluminium(I)

Cuijuan Zhang, Fabian Dankert, Ziang Jiang, Baolu Wang, Dominik Munz, and Jiaxiang Chu**

Abstract: The C–C bond formation between C1 molecules plays an important role in chemistry as manifested by the Fischer–Tropsch (FT) process. Serving as models for the FT process, we report here the reactions between a neutral Al^{I} complex (^{Me}NacNac)Al (**1**, ^{Me}NacNac = HC[(CMe)(NDipp)]$_2$, Dipp = 2,6-diisopropylphenyl) and various isocyanides. The step-by-step coupling mechanism was studied in detail by low-temperature NMR monitoring, isotopic labeling, as well as quantum chemical calculations. Three different products were isolated in reaction of **1** with the sterically encumbered 2,6-bis(benzhydryl)-4-Me-phenyl isocyanide (BhpNC). These products substantiate carbene intermediates. The reaction between **1** and adamantyl isocyanide (AdNC) generated a trimerization product, and a corresponding carbene intermediate could be trapped in the form of a molybdenum(0) complex. Tri-, tetra-, and even pentamerization products were isolated with the sterically less congested phenyl and *p*-methoxyphenyl isocyanides (PhNC and PMPNC) with concurrent construction of quinoline or indole heterocycles. Overall, this study provides evidence for carbene intermediates in FT-type chemistry of aluminium(I) and isocyanides.

Introduction

The transformation of C1 feedstocks (CO, CO_2, CH_4, CH_3OH, etc.) into fuels or chemical building-blocks stands amongst the most significant challenges in chemistry, particularly due to the growing demand for alternative resources other than petroleum.[1] The prime example of C1 chemistry is the Fischer–Tropsch (FT) process, which transforms CO to light hydrocarbons.[2] During this process, the interplay of C–O bond cleavage and C–C bond formation determines the product distribution. Whereas the detailed mechanism for this CO coupling reaction remains to be elucidated, carbenes have been proposed as the key intermediates based on in situ spectroscopy and density functional theory (DFT) calculations.[3] Furthermore, molecular complexes have been utilized to pinpoint the mechanism of CO couplings by taking advantage of their tunable structures and comparatively facile characterization.[4–6] Free carbene intermediates have been proposed for several such C–C bond formations mediated by main group elements.[6–9] For example, Stephan and co-workers reported the reaction between a group 1 phosphide[7] or amide[8] with CO to generate transient carbene species (**I**; Figure 1, a), although none of them could be isolated. In addition, a very limited number of metal-stabilized carbenes have been isolated in CO coupling reactions mediated by *f*- and *d*-block metals.[10–14] Marks' pioneering work featuring the reaction of a thorium neopentyl complex with CO resulted in the isolation of a thorium alkyl oxycarbene complex (**II**; Figure 1, a).[10–12] Scandium and samarium boryl oxycarbene complexes were obtained by Hou and co-workers via the reaction of metal boryl complexes with CO (**III** and **IV**; Figure 1, a).[13,14] These are rare examples that *CO-derived*

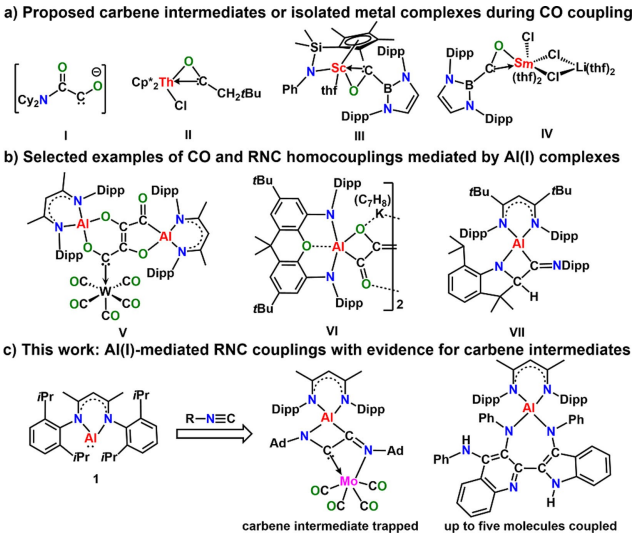

Figure 1. Selected examples of CO and RNC activation relevant to the current study as well as our work.

[*] Dr. C. Zhang, Z. Jiang, B. Wang, Prof. Dr. J. Chu
School of Chemical Sciences, University of Chinese Academy of Sciences
101408 Beijing (China)
E-mail: chujx@ucas.ac.cn
Dr. F. Dankert, Prof. Dr. D. Munz
Coordination Chemistry, Saarland University
Campus C4.1, 66123 Saarbrücken (Germany)
E-mail: dominik.munz@uni-saarland.de

carbene complexes could further react with CO to generate C–C bond coupling products, thus suggesting their intermediacy in the FT process.[15–18]

Isocyanides are isoelectronic with carbon monoxide and, thus, find extensive application in related chemical transformations.[19] As for FT-type homocouplings, isocyanides may oligomerize (e.g., trimerization,[20–23] tetramerization,[24–26] and pentamerization[27,28]) or even polymerize[29] in the presence of suitable catalysts. Whereas isocyanide-derived free carbenes have been proposed in some of these C–C bond formation processes,[21,23,24,26] as far as we know, they have never been isolated or trapped.

In light of aluminium's earth-abundancy, monovalent aluminium reagents have attracted much attention for the activation of small molecules.[30–34] However, their applications in CO and RNC homocoupling are just in the infancy. For instance, CO coupling products were obtained via transition-metal/main-group element cooperation with a neutral Al^I complex (^{Me}NacNac)Al (**1**, ^{Me}NacNac = HC[(CMe)(NDipp)]$_2$, Dipp = 2,6-diisopropylphenyl)[35] as the main group partner (selected example: **V**; Figure 1, b).[16,17] In addition, anionic Al^I complexes have also been shown to mediate four-, five-, or six-molecule coupling of CO (selected structure: **VI**; Figure 1, b).[9,36] Isocyanide coupling by Al^I remains largely unexplored,[37,38] yet it has been shown that (^{tBu}NacNac)Al (^{tBu}NacNac = HC[(C*t*Bu)(NDipp)]$_2$) generates bimolecular coupling products in reaction with DippNC (**VII**; Figure 1, b).

Herein, we report a comprehensive study on the mechanism of isocyanide homologation by **1**, thus serving as a model for the low valent metal centers present in the FT process (Figure 1, c). Based on the study of various isocyanide substituents and trapping experiments as well as quantum chemical calculations, we provide evidence for transient carbenes being the key intermediates in chain-propagation.

Results and Discussion

Encouraged by the applications of sterically encumbered substituents in the stabilization of reactive species, an isocyanide with a bulky Bhp group (Bhp = 2,6-bis(benzhydryl)-4-Me-phenyl) was selected for the initial studies. Monitoring the reaction between **1** and various ratios of BhpN^{13}C in 2-methyltetrahydrofuran (MeTHF), THF or hexane by ^{13}C NMR spectroscopy indicated the generation of a mixture of three products. Each of them was isolated under optimized conditions (Figure 2; for more details, see Table S1).

Mixing **1** and BhpN^{13}C in a 3.8:1 ratio in MeTHF at room temperature led to the appearance of a major signal at 75.7 ppm in the ^{13}C NMR spectrum (Figure S16). The reaction in THF gave the same major product, which converted to an intractable mixture within a few minutes. The reaction was scaled up in MeTHF, and the aluminaaziridine complex **2** was then isolated in 30% yield (based on BhpNC) as a red-brown powder. The low isolated yield is due to the generation of several side products, thus requiring

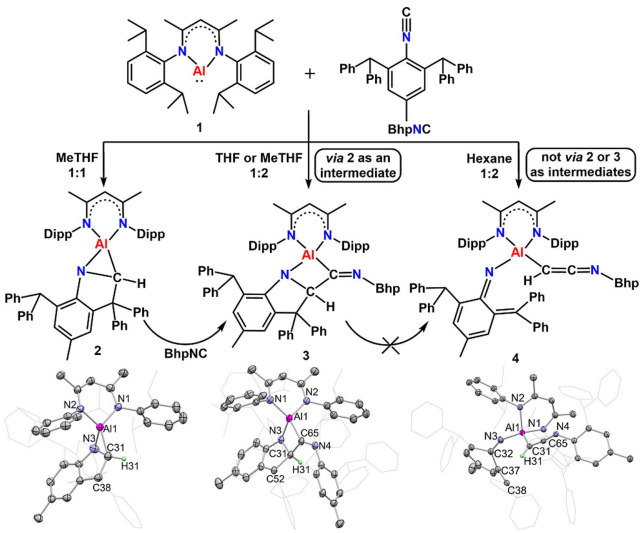

Figure 2. Reactions between **1** and BhpNC generate a mixture of three products, namely aluminaaziridine **2**, bimolecular coupling products **3** and **4**. Each of them were isolated under optimized (solvent, stoichiometry) conditions. Solid state structures are given with 50% probability ellipsoids; solvent and most H atoms are omitted for clarity.

an excess of **1** in the reaction mixture. The same observation was made in the syntheses of **3** and **4** (see below). Single crystals suitable for X-ray diffraction (SC-XRD) studies were obtained by slow evaporation of a hexane solution of **2** at room temperature.[39] In the AlNC three-membered ring, the Al–C31 (1.917(3) Å) bond length is similar to those in aluminacyclopropane complexes (1.91–1.99 Å),[40] while the Al–N3 and C31–N3 bond lengths (1.810(2) and 1.571(3) Å, respectively) fall within the typical range of Al–N and C–N single bonds. Comparing the ^{1}H NMR spectra of **2** and ^{13}C-labeled **2** (Figure S15), the proton on the AlNC ring was confirmed at 4.11 ppm with $^1J_{C-H}$ coupling of 140.8 Hz with the adjacent carbon atom at 75.7 ppm (Figure S18). The same coupling constant was found in the proton-coupled ^{13}C NMR spectrum (Figure S17). As opposed to the usually observed *end-on* coordination in monomeric isocyanide complexes,[41] the structure of **2** suggests a *side-on* coordination of BhpNC, giving rise to the aluminaazacyclopropene **A** (Figure 3a) prior to intramolecular C–H bond insertion. Unlike other low-valent main group centers, a coordination complex of Al^I with an isocyanide has not yet been isolated.[19] Whereas attempts to pinpoint this intermediate by ^{1}H and ^{13}C NMR spectroscopy at −70 °C failed (Figures S19 and S20), quantum chemical calculations (DLPNO-CCSD(T)/def2-TZVPP//r^{2}SCAN-3c with correction for solvation in THF, Figure S92; *cf.* Figure 6 for PhNC) suggest that end-on coordinated **1**-η^1-BhpNC ($\Delta G = 0$ kJ mol^{-1}) is more stable than the side-on coordinated **1**-η^2-BhpNC ($\Delta G = +45$ kJ mol^{-1}). However, the computed isomerization barrier is only moderate ($\Delta G^{\ddagger} = +82$ kJ mol^{-1}) and, thus, suggests a swift equilibrium at and below room temperature. The electronic structure of ylidic **A** is best understood in the form of the aluminaazacarbene **A′** (Figure 3a) according to a Mayer bond order of 0.94 for the C–N bond (r^{2}SCAN-3c),

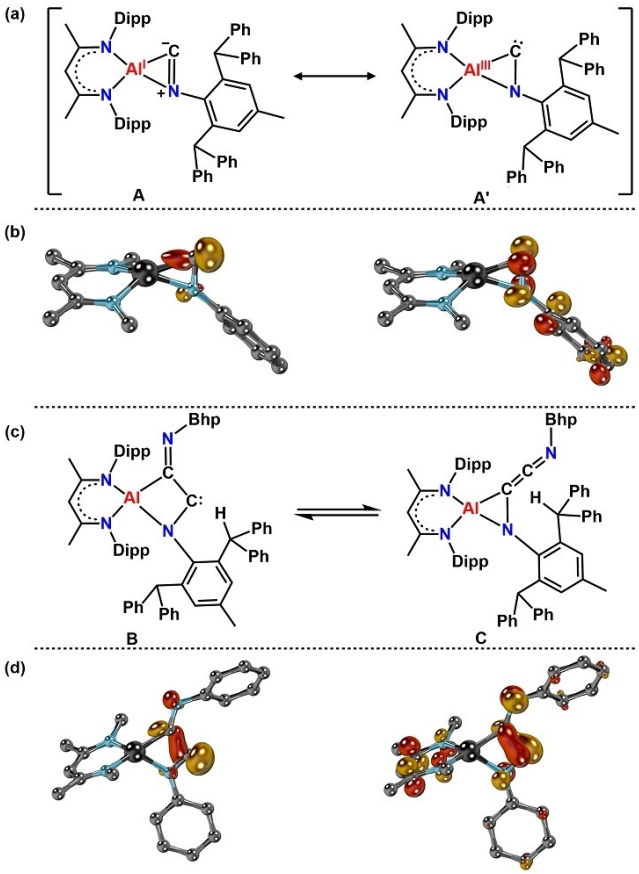

Figure 3. Proposed intermediates during the reactions of **1** and BhpNC to generate **2**–**4**. (a) Proposed intermediate for the generation of **2**, namely a side-on coordinated **1**-η^2-BhpNC intermediate with resonance structures **A** and **A′**. (b) Canonical Orbitals of the Al–N–C three-membered ring of **A′** showing the carbene lone-pair (left) and vacant π* molecular orbital between N and the carbene C (right). (c) Proposed intermediates during the reaction of **1** and 2 equiv. of BhpNC in hydrocarbon solvents, with **B** responsible for the generation of **3** and **C** responsible for the generation of **4**. (d) Canonical orbitals of the Al–N–C–C four-membered ring in the intermediate **B** showing the carbene lone-pair (left) and vacant π* molecular orbital between N and the carbene C (right). Aromatic substituents and H atoms are truncated for clarity in (b) and (d), yet have been included in the calculations.

which is well in line with the small singlet/triplet energy gap of $+157\,kJ\,mol^{-1}$. Plotting the molecular orbitals further substantiates the presence of an electron lone pair as well as a π* molecular orbital akin to the one found in carbenes (Figure 3b).[42] Notably, three-membered cyclic carbenes are highly reactive and exceedingly rare with only diaminocyclopropenylidenes having been isolated to date.[43] However, a related isocyanide-borylene adduct [(CN*t*Bu)B(IMe)(*t*Bu)] (IMe = :C(NMeCH)$_2$) was recently proposed computationally by Braunschweig and co-workers,[44] and described as a singlet carbene with a singlet/triplet energy gap of $+205\,kJ\,mol^{-1}$.

Switching the ratio of **1** and BhpN^{13}C to 1:1 in THF or MeTHF and monitoring the reaction by ^{13}C NMR spectroscopy at room temperature revealed the formation of another product with two ^{13}C NMR resonances at 210.9 and 88.9 ppm (Figure S25). The reaction was scaled up and the aluminaazacyclobutane **3** was isolated as a yellow powder in 50 % yield based on BhpNC (Figure 2). Single crystals of **3** suitable for SC-XRD studies were obtained by slow evaporation of a hexane solution at room temperature. The formation of **3** via an isocyanide dimerization/C–H activation sequence is peculiar, and similar metal-mediated transformations have hitherto only been reported by Cui et al..[19,37] Both the Al–C65 and Al–N3 bond lengths (2.027(2) and 1.8272(19) Å, respectively) in **3** are similar to those reported by Cui et al. (2.003(5) and 1.818(4) Å, respectively). Comparing the ^{1}H NMR spectra of **3** and ^{13}C-labeled **3** reveals that the proton within the AlNC2 ring resonates at 5.24 ppm (J_{C-H} = 142.6 and 2.0 Hz, Figure S24; for the ^{13}C NMR spectrum, see Figure S26). We further studied the mechanism for the generation of **3**. In order to pinpoint the alleged intermediacy of the AlNC2 four-membered cyclic carbene **B** (Figure 3c), we monitored the reaction between **1** and BhpN^{13}C at −70 °C in THF-d_8 by ^{1}H and ^{13}C NMR spectroscopy. However, the instantaneous formation of **2** was observed even in the cold, followed by subsequent transformation to **3** upon elevating the temperature. As such, we conclude that **2** serves as precursor of **3** in THF (Figure S28 and S29; note that **3** was generated via a different mechanism when the reaction was performed in hydrocarbon solvents, see below). Indeed, this was further confirmed by the reaction between **2** and BhpNC, where **3** is generated as the major product (Figure S30).

Interestingly, when the reaction between **1** and BhpN^{13}C was performed in a ca. 1:1 ratio in hexane at room temperature, compound **3** was generated as a minor product, with the major product (**4**) featuring two resonances at 176.3 and 28.1 ppm in the ^{13}C NMR spectrum (Figure S36). Compound **4** was then isolated as a red-brown solid in 25 % yield from hexane. Single crystals suitable for SC-XRD studies were obtained by evaporation techniques from hexane and **4** was identified as an azaallenyl ketimide complex (Figure 2). The C31–C65 (1.2994(17) Å) and C65–N4 bond lengths (1.2260(16) Å) as well as the C31–C65–N4 bond angle (172.69(12)°) of the azaallenyl ligand are similar to those in the only other known metal azaallenyl complex with hydrogen substituent on the α-carbon, namely [(PNP)(ODipp)Nb(=O)(CH=C=N*t*Bu)] (1.314(4) Å, 1.235(4) Å, and 170.9(3)°, respectively, PNP$^-$=N[2-P*i*Pr$_2$-4-methylphenyl]$_2^-$).[45] The C32–N3 (1.2649 (17) Å) and C37–C38 (1.3705(18) Å) bond lengths in the ketimide ligand also fall in the ranges of typical C=N and C=C double bonds. Through comparing the ^{1}H NMR spectra of **4** and ^{13}C-labeled **4**, the proton on the azaallenyl ligand (*H*C=C=N) was located at 1.35 ppm ($^1J_{C-H}$ = 136.0 Hz; see Figure S34 and S38). Note that although deoxygenative homocoupling of CO with the formation of a ketene group (C=C=O) has been documented using low valent Ta,[46] Mo,[47,48] or Si[49] complexes, the overall denitrogenative homocoupling of isocyanides is largely elusive and was only recently achieved using a silylene-bridged nickel cluster[50] and an alumaborane featuring an electron-precise Al–B bond.[51]

The generation of both **3** and **4** in *hydrocarbon* solvents raised the question of whether **3** was an intermediate during the formation of **4**. However, we found that **3** could not transform to **4** at room temperature or at elevated temperatures. We furthermore wondered whether **2** serves as intermediate for the generation of **3** or **4** in these hydrocarbon solvents. Therefore, a variable temperature (VT) NMR experiment was carried out. When the reaction between **1** and BhpN^{13}C was performed at −70 °C in toluene-d_8 and monitored by ^{1}H and ^{13}C NMR spectroscopy, no intermediate was identified between −70 and −50 °C, while both compounds **3** and **4** started to form at −50 °C (Figure S39 and S40). Since we did not observe **2**, we conclude that **2** likely is not responsible for the generation of **3** and **4** in toluene-d_8 (note that **2** was an intermediate for the generation of **3** in THF, see above). Therefore, we tentatively propose that the generation of **3** in toluene may proceed via an AlNC2 four-membered cyclic carbene **B** followed by intramolecular C–H activation,[37] while the generation of **4** may involve intermediate **C**[52] followed by intramolecular C–H activation and subsequent C–N bond cleavage (Figure 3c and S41). Indeed, the computational analysis of the relative energies of intermediates **B** and **C** with phenyl substituents suggests that they coexist in solution (see below).

We were particularly intrigued by the carbene intermediate **B** and a series of trapping experiments were conducted. Unfortunately, all attempts with Se, CuCl, $Mo(CO)_6$ or AdNC proved unproductive (Figure S42–S51). However, its electronic structure was elucidated by DFT. According to the Mayer Bond order of 1.36 for the N–C bond, and 0.80 for the C–C bond in the four-membered ring (r^{2}SCAN-3c), and in combination with the frontier orbitals of the electron lone pair and π-system (Figure 3d), compound **B** is best understood as a push-pull carbene with an amino-donor and an imino-acceptor. Note that the isolation of imino-substituted carbenes remains hitherto elusive[53]—just as is the case for any acceptor-substituted free carbene.

Carbenes may react with isocyanides to generate ketenimines. We therefore hypothesized that the carbene intermediates such as **B** in Figure 3c may couple with another molecule of isocyanide. In order to prevent the intramolecular C–H insertion of these transient carbenes (see above), reactions with aliphatic isocyanides and aromatic isocyanides without *ortho*-substituents were performed. The reaction between **1** and 3 equiv. of adamantyl isocyanide (AdNC) in THF afforded bright yellow **5**, which was isolated in 62 % yield. The solid-state structure of single crystals of **5** obtained from a saturated ether solution confirmed the formation of the trimolecular coupling product, which features a rare (amino)(imino) scaffold and an exocyclic ketenimine (Figure 4). Notable is the co-planar AlNC2 four-membered ring (torsion angle of Al–N3–C31–C54: 4.65°). The C31–C42 (1.320(2) Å) and C42–N5 (1.234(2) Å) bond lengths and C31–C42–N5 bond angles (164.27(17)°) in the ketenimine ligand are similar to those in the azaallenyl ligand of **4**. The ^{13}C NMR spectrum of **5** features a resonance at 203.7 ppm corresponding to the imino group, and two resonances at 99.7 and 194.7 ppm

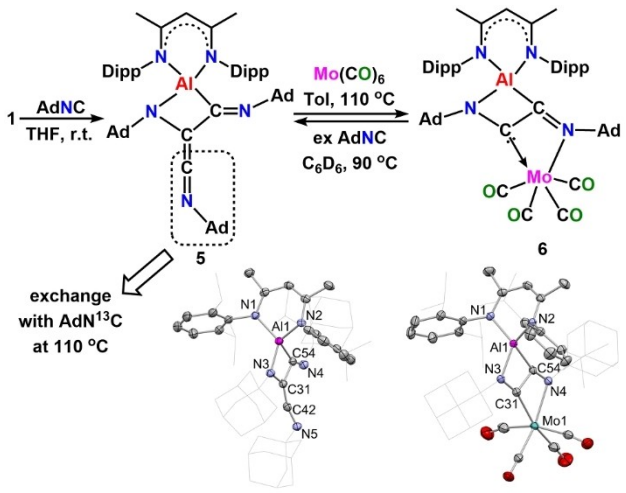

Figure 4. Reaction of **1** and AdNC to generate the trimolecular coupling product **5**, as well as the interconversion between **5** and **6**. Solid state structures are given with 50 % probability ellipsoids; solvent and H atoms are omitted for clarity.

corresponding to the ketenimine group. This reaction parallels the trimolecular coupling of isocyanides mediated by silylenes.[21,23] Monitoring the reaction between **1** and AdN^{13}C by ^{13}C NMR spectroscopy at −70 °C indicated the generation of an intermediate, which transformed to **5** at around −40 °C (Figure S56). Based on the similar ^{13}C NMR resonances of this intermediate and **5**, we tentatively assigned it as an isomer of **5** (Figure S57). All attempts to trap the carbene intermediate with CuCl or $Mo(CO)_6$ remained unsuccessful (Figure S58–S61).

However, mixing **5** and AdN^{13}C in toluene-d_8 and monitoring by ^{13}C NMR spectroscopy indicated the labeling of one of the carbons in the ketenimine group (C=*C*=NAd) after heating at 110 °C for two days (Figure S62–S63). The facile isocyanide exchange suggests a comparatively weak C=C bond in **5**. Encouraged by this, **5** was treated with $Mo(CO)_6$ to afford the orange-yellow molybdenum carbene complex **6** (Figure 4). The ^{13}C NMR spectrum of **6** exhibited a resonance at 290.4 ppm, a value consistent with Fischer-type carbene complexes.[54] SC-XRD studies confirmed **6** as a rare example of (amino)(imino)carbene complex. Notable is that, as opposed to the generation of carbenes from diazo or ketene compounds, the generation of free carbenes or carbene intermediates from ketenimines is exceedingly rare.[20] Contrary to the known (amino)(imino)carbene complexes where the carbenes acted as monodentate ligands,[44,55] the carbene unit in **6** is κ^2-coordinated through both $C_{carbene}$ and N_{imine} atoms (Mo–C31 and Mo–N4 distances in **6**: 2.240(2) and 2.3425(17) Å, respectively). The hemilabile coordination of donor groups in functionalized carbene ligands has been demonstrated before.[18,56] In addition, **6** could react with excess AdNC to regenerate **5**, thus confirming that (amino)(imino)carbenes are indeed viable intermediates during isocyanide coupling (Figure 4 and S67).[57] This result seems striking and parallels FT-type chemistry, where Marks[10–12] as well as Hou et al.[13,14]

proposed that *CO-derived* carbene complexes could further react with another equivalent of CO to generate C–C coupled products.[58]

The reaction of **1** with sterically less congested aryl isocyanides afforded products involving intramolecular phenyl C–H bond insertions. For the reaction with 3 equiv. of *p*-methoxyphenyl isocyanide (PMPNC) in hexane at room temperature, yellow crystals of **7** were isolated in 56 % yield. **7** was fully characterized, including SC-XRD studies, and remarkably features a quinoline group (Figure 5). The synthesis of quinolines has been of considerable research interest due to their applications as pharmaceuticals, agrochemicals, and functionalized materials.[59] The generation of **7** shows that the trimerization of isocyanides affords a complementary entry to quinoline synthesis. A plausible mechanism for the generation of **7** via an intermediate similar to **5** followed by intramolecular hydrogen transfer to the ketenimine group is demonstrated in Figure S70. Related mechanisms have been proposed for Ta-,[26] Nb-,[27] and Si-[21] mediated isocyanide coupling reactions. An intermolecular arene C–H bond activation by a Lewis acid-stabilized ketenimine was also reported.[60,61]

Different from the reaction between **1** and PMPNC which gave a trimerization product, the reaction between **1** and 4 equiv. of PhNC in hexane at room temperature gave a yellow solid (**8**), which was isolated in 52 % yield. **8** was fully characterized, and an SC-XRD experiment revealed a tetramolecular coupling product (Figure 5). Apparently, the methoxy donor group in the *para*-position switches the chemoselectivity (for a discussion of the mechanisms involved in the formation of **8**, see Figure S74). The reaction outcome between **1** and PhNC also depends on the reaction temperature. Reacting **8** with 1 equiv. of PhNC in toluene at 150 °C for 4 days generated a red powder (**9**). The solid-state structure of **9** features a quinoline ring and an indole ring connected by a C–C single bond (Figure 5). Compound **9** could also be generated from **1** and 6 equiv. of PhNC in toluene at 150 °C in one pot, thus realizing the construction of two important heterocycles from two simple substrates in a single step.

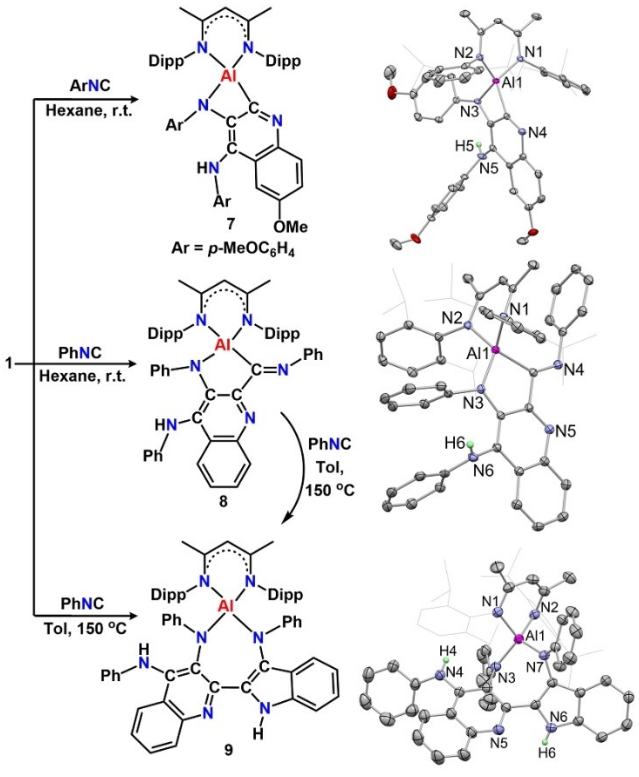

Figure 5. Reactions of **1** and PMPNC or PhNC to generate tri-, tetra-, and pentamolecular coupling products **7**–**9**. Solid state structures are given with 50 % probability ellipsoids; solvent and most H atoms are omitted for clarity.

Among all the isocyanides studied, only the reaction with PhNC gave tetra- and penta-molecular coupling products. Bearing in mind that tetra- and penta-molecular isocyanide coupling have been poorly understood in the literature,[24–28] the reaction between **1** and PhNC provides an opportunity to study the step-by-step chain growth computationally (Figure 6). The computations reveal the delicate interplay of three potentially competing pathways and, thus, elucidate why small adjustments of the experimental conditions lead to different synthetic outcomes. Most salient, they identify carbene $\mathbf{B^{Ph}}$ ($\Delta G = -90\ \mathrm{kJ\,mol^{-1}}$) as the key-intermediate in chain growth. This carbene forms after coordination of phenyl isocyanide to **1** giving $\mathbf{IM1^{Ph}}$ ($\Delta G = +43\ \mathrm{kJ\,mol^{-1}}$, $\Delta G^{\ddagger} = +60\ \mathrm{kJ\,mol^{-1}}$), subsequent association of a second molecule of isocyanide ($\mathbf{IM2^{Ph}}$; $\Delta G = +46\ \mathrm{kJ\,mol^{-1}}$), followed by reductive coupling ($\mathbf{IM3^{Ph}}$, $\Delta G = -8\ \mathrm{kJ\,mol^{-1}}$, $\Delta G^{\ddagger} = +52\ \mathrm{kJ\,mol^{-1}}$) and rearrangement ($\Delta G^{\ddagger} = (35+8)\ \mathrm{kJ\,mol^{-1}} = +43\ \mathrm{kJ\,mol^{-1}}$). This overall transformation is predicted to proceed swiftly at low temperatures with the highest barrier amounting to only $\Delta G^{\ddagger} = +52\ \mathrm{kJ\,mol^{-1}}$. The barriers for the pathway via carbene $\mathbf{A^{Ph}}$ ($\mathbf{TS[IM1^{Ph}\text{-}A^{Ph}]}$, $\Delta G^{\ddagger} = +118\ \mathrm{kJ\,mol^{-1}}$) or via $\mathbf{IM1^{Ph}}$ through [2+2] cycloaddition ($\mathbf{TS[IM1^{Ph}\text{-}B^{Ph}]}$, $\Delta G^{\ddagger} = +151\ \mathrm{kJ\,mol^{-1}}$) are not compatible with the experimentally observed kinetics. However, remember that intermediate **A** forms with the more sterically encumbered BhpNC (*cf.* Figure 3a; Figure S92), where the formation of $\mathbf{IM2^{Bhp}}$ is disfavored due to steric reasons.

Chain growth from $\mathbf{B^{Ph}}$ to $\mathbf{5^{Ph}}$ occurs concomitantly by two mechanisms. One is the direct coupling of the carbene $\mathbf{B^{Ph}}$ with another equivalent of phenyl isocyanide via $\mathbf{TS\text{-}[B^{Ph}\text{-}5^{Ph}]}$ with an overall barrier of $\Delta\Delta G^{\ddagger} = (-39+90)\ \mathrm{kJ\,mol^{-1}} = +51\ \mathrm{kJ\,mol^{-1}}$. Interestingly, this transition state is with a C–C distance of 2.54 Å similar to that in the Wanzlick-dimerization of carbenes.[62] Alternatively, carbene $\mathbf{B^{Ph}}$ isomerizes to $\mathbf{C^{Ph}}$ ($\Delta G = -109\ \mathrm{kJ\,mol^{-1}}$) via $\Delta\Delta G^{\ddagger} = (-43+90)\ \mathrm{kJ\,mol^{-1}} = +47\ \mathrm{kJ\,mol^{-1}}$, which is only 4 kJ mol^{-1} lower in energy. The subsequent coordination of phenyl isocyanide affords $\mathbf{IM4^{Ph}}$ reversibly ($\Delta G = -110\ \mathrm{kJ\,mol^{-1}}$) via $\mathbf{TS[C^{Ph}\text{-}IM4^{Ph}]}$ ($\Delta\Delta G^{\ddagger} = (-67+109)\ \mathrm{kJ\,mol^{-1}} = +42\ \mathrm{kJ\,mol^{-1}}$). $\mathbf{5^{Ph}}$ is obtained via migratory insertion transition state $\mathbf{TS[IM4^{Ph}\text{-}5^{Ph}]}$ with $\Delta\Delta G^{\ddagger} = (-98\ \mathrm{kJ\,mol^{-1}} + 110\ \mathrm{kJ\,mol^{-1}}) = +12\ \mathrm{kJ\,mol^{-1}}$. The C–C distance of 2.56 Å in $\mathbf{TS[IM4^{Ph}\text{-}5^{Ph}]}$ is only marginally longer as found for $\mathbf{TS[B^{Ph}\text{-}5^{Ph}]}$, also highlighting its carbene character (see above). The coexistence of two mechanisms via $\mathbf{B^{Ph}}$ and $\mathbf{C^{Ph}}$ recalls the generation of

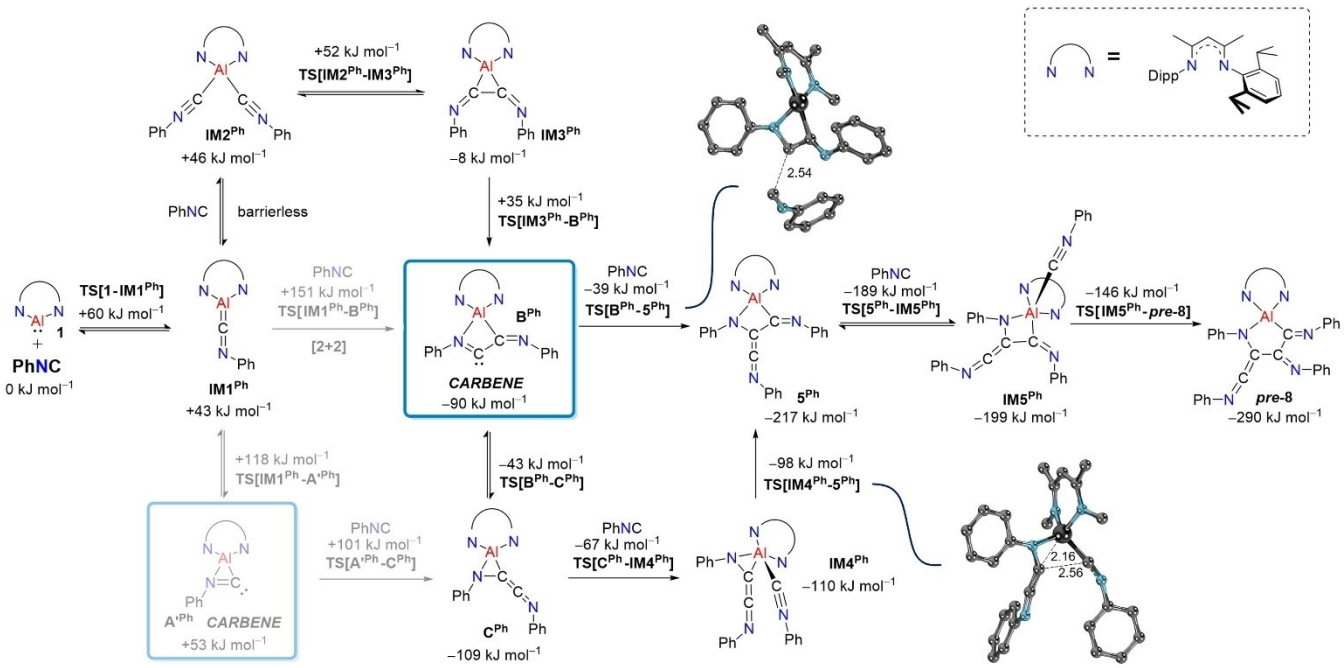

Figure 6. Computed energy profile (DLPNO-CCSD(T)/def2-TZVPP//r^2SCAN-3c) for the homologation of phenyl isocyanide under inclusion of solvation effects in benzene. Energy values relate to ΔG ($\Delta G^{\ddagger}$, respectively) in respect to **1** and **PhNC**, distances are given in [Å]. For the reaction of **1** and BhpNC, see Figure S92; for the reaction of **1** and PhNC in THF, see Figure S93.

both **3** and **4** in toluene via $\mathbf{B^{Bhp}}$ and $\mathbf{C^{Bhp}}$, respectively (Figure 3c).

Subsequently, trimer $\mathbf{5^{Ph}}$ may convert to the tetramer ***pre*-8** ($\Delta G = -290\ \mathrm{kJ\,mol^{-1}}$) via another association (**IM5^{Ph}**; $\Delta G = -199\ \mathrm{kJ\,mol^{-1}}$, $\Delta G^{\ddagger} = (-189+217)\ \mathrm{kJ\,mol^{-1}} = +28\ \mathrm{kJ\,mol^{-1}}$)—migratory insertion (**TS[IM5^{Ph}-*pre*-8]**; $\Delta G^{\ddagger} = (-146+217)\ \mathrm{kJ\,mol^{-1}} = +71\ \mathrm{kJ\,mol^{-1}}$) sequence. The tetramer ***pre*-8** then serves as the precursor to the C–H insertion products **8** and **9** (*cf.* Figure 5). Akin to the reactivity of strongly ambiphilic iminocarbenes,[53] the formation of **8** ($\Delta G = -496\ \mathrm{kJ\,mol^{-1}}$) likely proceeds via electrophilic attack at the phenyl ring (**TS(pre8-IM6^{Ph})** to generate intermediate **IM6^{Ph}** ($\Delta G = -262\ \mathrm{kJ\,mol^{-1}}$, $\Delta G^{\ddagger} = (-227+290)\ \mathrm{kJ\,mol^{-1}} = +63\ \mathrm{kJ\,mol^{-1}}$), followed by rate-limiting ($\Delta G^{\ddagger} = (-290+167)\ \mathrm{kJ\,mol^{-1}} = +123\ \mathrm{kJ\,mol^{-1}}$) proton transfer involving PhNC (Figure 7; see Figure S97 for the intramolecular 1,3-proton shift to yield **8**, which proceeds with $\Delta G^{\ddagger} = +141\ \mathrm{kJ\,mol^{-1}}$).

The conversion of **8** to **9** (Figure S98) parallels the pathway depicted in Figures 6 and 7. Analogous to the rearrangement of $\mathbf{C^{Ph}}$ to $\mathbf{B^{Ph}}$, **8** isomerizes to a transient carbene. This carbene intermediate binds PhNC and eventually forms **9** via subsequent electrophilic attack at the phenyl ring and proton transfer. Therefore, the successful isolation of a diversity of homologation (including novel tetra- and pentamerization) products can be attributed to the presence of a suitable ambiphilic metal center, appropriate choice of substituents on the isocyanide, and careful control of reaction conditions.

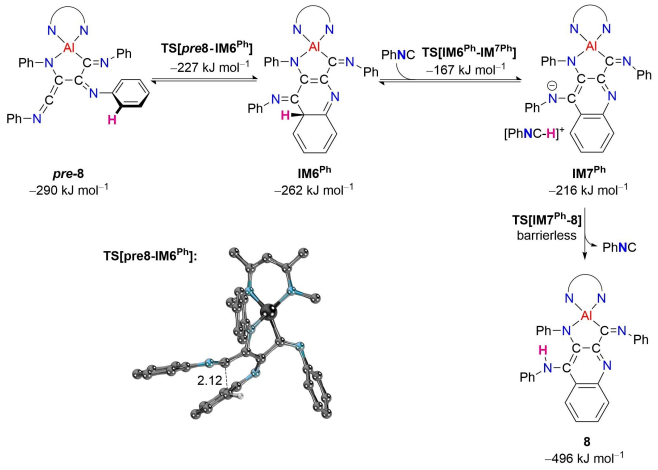

Figure 7. Computed energy profile (DLPNO-CCSD(T)/def2-TZVPP//r^2SCAN-3c) for the formation of **8** from ***pre*-8** under inclusion of solvation effects in benzene. Energy values relate to ΔG ($\Delta G^{\ddagger}$, respectively) in respect to **1** and PhNC, distance is given in [Å].

Conclusion

In summary, we have investigated in detail the reactions between the Al^{I} complex **1** and isocyanides with various substituents. The sterically encumbered BhpNC gave the three products **2**–**4**, each of which can be isolated under optimized conditions. They indicate that two different kinds of carbene intermediates may be generated during the reaction of **1** and BhpNC. The reaction with AdNC generated the (amino)(imino) complex **5** with an exocyclic

ketenimine group, which converts with $Mo(CO)_6$ to the (amino)(imino)carbene complex **6** under the release of isocyanide. The latter is the hitherto first isolated carbene complex involved in isocyanide homologations. The reactions with sterically less congested aryl isocyanides (PMPNC and PhNC) constructed quinoline or indole rings (**7**–**9**) by three-, four-, or a rare five-molecular coupling. The chain growth mechanism was elucidated by computations, which reveal a delicate balance of various pathways and highlight carbenes as key intermediates for chain growth. Altogether, these in-depth experimental and computational studies provide a step-by-step mechanism for the intriguing yet poorly understood isocyanide homologation[25–27] and build a bridge between molecular carbene chemistry and the Fischer–Tropsch process. Overall, our work stimulates the discovery of new organic transformations involving CO or isocyanides mediated by main group elements and transition metals.

Acknowledgements

J. C. gratefully acknowledge the supported from the Natural Science Foundation of China (No. 22001249) and the Chinese Academy of Sciences. J. C. and C. Z. also acknowledge the support from the Fundamental Research Funds for the Central Universities. D. M. and F. D. gratefully acknowledge the scientific support and HPC resources provided by the Erlangen National High Performance Computing Center (NHR@FAU) of the Friedrich-Alexander-Universität Erlangen-Nürnberg (FAU) under the NHR project n100af. NHR funding is provided by federal and Bavarian state authorities. NHR@FAU hardware is partially funded by the German Research Foundation (DFG)—440719683. This project has received cofunding from the European Research Council (ERC) under the Horizon 2020 research and innovation programme (PUSH-IT, 948185). We thank Prof. Gabriel Ménard from the University of Calgary, Prof. Jiliang Zhou from Sichuan University, Dr. Mikiyas Assefa from University of Southern California, and Dr. Leiyang Zhang from the University of Chinese Academy of Sciences for insightful discussions. Open Access funding enabled and organized by Projekt DEAL.

Conflict of Interest

The authors declare no conflict of interest.

Data Availability Statement

The data that support the findings of this study are available in the supplementary material of this article.

Keywords: Aluminum · Carbene · Fischer–Tropsch · Homologation · Isocyanide

[1] X. F. Wu, B. X. Han, K. L. Ding, Z. M. Liu, in *The Chemical Transformations of C1 Compounds*, Wiley-VCH, Weinheim, **2022**.
[2] B. H. Davis, M. L. Occelli, *Advances in Fischer–Tropsch synthesis, catalysts, and catalysis*, CRC press, Boca Raton, **2009**.
[3] K. T. Rommens, M. Saeys, *Chem. Rev.* **2023**, *123*, 5798-5858.
[4] N. M. West, A. J. M. Miller, J. A. Labinger, J. E. Bercaw, *Coord. Chem. Rev.* **2011**, *255*, 881–898.
[5] R. Y. Kong, M. R. Crimmin, *Dalton Trans.* **2020**, *49*, 16587–16597.
[6] S. Fujimori, S. Inoue, *J. Am. Chem. Soc.* **2022**, *144*, 2034–2050.
[7] M. T. Xu, A. R. Jupp, D. W. Stephan, *Angew. Chem. Int. Ed.* **2019**, *58*, 3548–3552.
[8] M. T. Xu, Z. W. Qu, S. Grimme, D. W. Stephan, *J. Am. Chem. Soc.* **2021**, *143*, 634–638.
[9] A. Heilmann, M. M. D. Roy, A. E. Crumpton, L. P. Griffin, J. Hicks, J. M. Goicoechea, S. Aldridge, *J. Am. Chem. Soc.* **2022**, *144*, 12942–12953.
[10] P. J. Fagan, J. M. Manriquez, T. J. Marks, V. W. Day, S. H. Vollmer, C. S. Day, *J. Am. Chem. Soc.* **1980**, *102*, 5393–5396.
[11] K. G. Moloy, T. J. Marks, V. W. Day, *J. Am. Chem. Soc.* **1983**, *105*, 5696–5698.
[12] K. G. Moloy, P. J. Fagan, J. M. Manriquez, T. J. Marks, *J. Am. Chem. Soc.* **1986**, *108*, 56–67.
[13] B. L. Wang, X. H. Kang, M. Nishiura, Y. Luo, Z. M. Hou, *Chem. Sci.* **2016**, *7*, 803–809.
[14] B. L. Wang, G. Luo, M. Nishiura, Y. Luo, Z. M. Hou, *J. Am. Chem. Soc.* **2017**, *139*, 16967–16973.
[15] Crimmin and co-workers demonstrated that CO-derived transitional metal carbene complexes can engage in subsequent C–C bond formations. These reactions occur at the Al-C bonds instead of the M=C bonds (see refs. [16] and [17]). They also showed that these carbene complexes react with H_2 to produce well-defined products containing methylene groups (see ref. [18]).
[16] R. Y. Kong, M. R. Crimmin, *J. Am. Chem. Soc.* **2018**, *140*, 13614–13617.
[17] R. Y. Kong, M. Batuecas, M. R. Crimmin, *Chem. Sci.* **2021**, *12*, 14845–14854.
[18] M. Batuecas, R. Y. Kong, A. J. P. White, M. R. Crimmin, *Angew. Chem. Int. Ed.* **2022**, *61*, e202202241.
[19] S. Mukhopadhyay, A. G. Patro, R. S. Vadavi, S. Nembenna, *Eur. J. Inorg. Chem.* **2022**, e202200469.
[20] C. Valero, M. Grehl, D. Wingbermühle, L. Kloppenburg, D. Carpenetti, G. Erker, J. L. Petersen, *Organometallics* **1994**, *13*, 415–417.
[21] Y. Xiong, S. L. Yao, M. Driess, *Chem. Eur. J.* **2009**, *15*, 8542–8547.
[22] Z. D. Brown, P. Vasko, J. D. Erickson, J. C. Fettinger, H. M. Tuononen, P. P. Power, *J. Am. Chem. Soc.* **2013**, *135*, 6257–6261.
[23] Y. L. Zhao, Y. L. Chen, L. Zhang, J. C. Li, Y. B. Peng, Z. K. Chen, L. Y. Jiang, H. P. Zhu, *Inorg. Chem.* **2022**, *61*, 5215–5223.
[24] S. Hasegawa, Y. Ishida, H. Kawaguchi, *Chem. Commun.* **2021**, *57*, 8296–8299.
[25] J. M. Shen, G. P. A. Yap, K. H. Theopold, *J. Am. Chem. Soc.* **2014**, *136*, 3382–3384.
[26] L. Xiang, Z. W. Xie, *Organometallics* **2016**, *35*, 233–241.
[27] B. M. Kriegel, R. G. Bergman, J. Arnold, *J. Am. Chem. Soc.* **2016**, *138*, 52–55.
[28] T. Tanase, T. Ohizumi, K. Kobayashi, Y. Yamamoto, *Organometallics* **1996**, *15*, 3404–3411.
[29] C. R. Cahoon, C. W. Bielawski, *Coord. Chem. Rev.* **2018**, *374*, 261–278.

[30] Y. S. Liu, J. Li, X. L. Ma, Z. Yang, H. W. Roesky, *Coord. Chem. Rev.* **2018**, *374*, 387–415.
[31] J. Hicks, P. Vasko, J. M. Goicoechea, S. Aldridge, *Angew. Chem. Int. Ed.* **2021**, *60*, 1702–1713.
[32] M. P. Coles, M. J. Evans, *Chem. Commun.* **2023**, *59*, 503–519.
[33] X. Zhang, Y. B. Mei, L. L. Liu, *Chem. Eur. J.* **2022**, *28*, e202202102.
[34] F. Dankert, C. Hering-Junghans, *Chem. Commun.* **2022**, *58*, 1242–1262.
[35] C. M. Cui, H. W. Roesky, H.-G. Schmidt, M. Noltemeyer, H. Hao, F. Cimpoesu, *Angew. Chem. Int. Ed.* **2000**, *39*, 4274–4276.
[36] M. J. Evans, M. G. Gardiner, M. D. Anker, M. P. Coles, *Chem. Commun.* **2022**, *58*, 5833–5836.
[37] X. F. Li, X. Y. Cheng, H. B. Song, C. M. Cui, *Organometallics* **2007**, *26*, 1039–1043.
[38] M. J. Evans, M. D. Anker, C. L. McMullin, M. P. Coles, *Chem. Sci.* **2023**, *14*, 6278–6288.
[39] Deposition numbers 2251192 (for **2**), 2251193 (for **3**), 2251194 (for **4**), 2251195 (for **5**), 2251196 (for **6**), 2251197 (for **7**), 2251198 (for **8**), 2251199 (for **9**), 2264529 (for **10**), and 2251200 (for BhpNC) contain the supplementary crystallographic data for this paper. These data are provided free of charge by the joint Cambridge Crystallographic Data Centre and Fachinformationszentrum Karlsruhe Access Structures service.
[40] C. Bakewell, A. J. P. White, M. R. Crimmin, *Chem. Sci.* **2019**, *10*, 2452–2458.
[41] E. Singleton, H. E. Oosthuizen, in *Metal Isocyanide Complexes. In Advances in Organometallic Chemistry, Vol. 22* (Eds.: F. G. A. Stone, R. West), Academic Press, San Diego, **1983**, pp. 209–310.
[42] K. Breitwieser, H. Bahmann, R. Weiss, D. Munz, *Angew. Chem. Int. Ed.* **2022**, *61*, e202206390.
[43] V. Lavallo, Y. Canac, B. Donnadieu, W. W. Schoeller, G. Bertrand, *Science* **2006**, *312*, 722–724.
[44] H. Braunschweig, W. C. Ewing, K. Ferkinghoff, A. Hermann, T. Kramer, R. Shang, E. Siedler, C. Werner, *Chem. Commun.* **2015**, *51*, 13032–13035.
[45] T. Kurogi, B. Pinter, D. J. Mindiola, *Organometallics* **2018**, *37*, 3385–3388.
[46] D. R. Neithamer, R. E. LaPointe, R. A. Wheeler, D. S. Richeson, G. D. Van Duyne, P. T. Wolczanski, *J. Am. Chem. Soc.* **1989**, *111*, 9056–9072.
[47] J. A. Buss, T. Agapie, *Nature* **2016**, *529*, 72–75.
[48] J. A. Buss, T. Agapie, *J. Am. Chem. Soc.* **2016**, *138*, 16466–16477.
[49] Y. W. Wang, A. Kostenko, T. J. Hadlington, M.-P. Luecke, S. L. Yao, M. Driess, *J. Am. Chem. Soc.* **2019**, *141*, 626–634.
[50] K. Shimamoto, Y. Sunada, *Chem. Sci.* **2022**, *13*, 4115–4121.
[51] Z. Güven, L. Denker, D. Wullschläger, J. P. Martínez, B. Trzaskowski, R. Frank, *Angew. Chem. Int. Ed.* **2022**, *61*, e202209502.
[52] S. L. Staun, G. T. Kent, A. Gomez-Torres, G. Wu, S. Fortier, T. W. Hayton, *Organometallics* **2021**, *40*, 2934–2938.
[53] Y. K. Loh, M. Melaimi, D. Munz, G. Bertrand, *J. Am. Chem. Soc.* **2023**, *145*, 2064–2069.
[54] D. Munz, *Organometallics* **2018**, *37*, 275–289.
[55] H. Braunschweig, T. Herbst, K. Radacki, C. W. Tate, A. Vargas, *Chem. Commun.* **2013**, *49*, 1702–1704.
[56] J. X. Chu, D. Munz, R. Jazzar, M. Melaimi, G. Bertrand, *J. Am. Chem. Soc.* **2016**, *138*, 7884–7887.
[57] Reactions of **5** with other isocyanides were conducted as well. They reveal that **5** reacts with PhNC and CyNC with the release of one molecule of AdNC. Additional rearrangements occur. Details will be reported in due course.
[58] A series of experiments were performed to determine if isocyanide-derived carbenes react with H_2. The reactions between **6** and H_2 gave a major product (**10**), whereas **5** proved unreactive. For more details, see sections 2.12 and 2.13 in the Supporting Information.
[59] C. Teja, F. R. N. Khan, *Chem. Asian J.* **2020**, *15*, 4153–4167.
[60] J. Surkau, K. Bläsing, J. Bresien, D. Michalik, A. Villinger, A. Schulz, *Chem. Eur. J.* **2022**, *28*, e202201905.
[61] For another mechanism for the formation of compound **7** involving cycloaddition and tautomerization, see Figure S71.
[62] J. Messelberger, M. Kumar, S. J. Goodner, D. Munz, *Org. Chem. Front.* **2021**, *8*, 6663–6669.

Manuscript received: May 25, 2023
Accepted manuscript online: June 15, 2023
Version of record online: June 15, 2023